ChemPubSoc Europe

DOI: 10.1002/chem.201403241

CHEMISTRY
A European Journal
Communication

Lanthanides

Highly Selective Water Adsorption in a Lanthanum Metal–Organic Framework

Raoul Plessius,[a] Rosa Kromhout,[a] André Luis Dantas Ramos,[a, b] Marilena Ferbinteanu,[c] Marjo C. Mittelmeijer-Hazeleger,[a] Rajamani Krishna,[a] Gadi Rothenberg,[a] and Stefania Tanase*[a]

Abstract: We present a new metal–organic framework (MOF) built from lanthanum and pyrazine-2,5-dicarboxylate (pyzdc) ions. This MOF, $[La(pyzdc)_{1.5}(H_2O)_2]\cdot 2H_2O$, is microporous, with 1D channels that easily accommodate water molecules. Its framework is highly robust to dehydration/hydration cycles. Unusually for a MOF, it also features a high hydrothermal stability. This makes it an ideal candidate for air drying as well as for separating water/alcohol mixtures. The ability of the activated MOF to adsorb water selectively was evaluated by means of thermogravimetric analysis, powder and single-crystal X-ray diffraction and adsorption studies, indicating a maximum uptake of 1.2 mmol g^{-1} MOF. These results are in agreement with the microporous structure, which permits only water molecules to enter the channels (alcohols, including methanol, are simply too large). Transient breakthrough simulations using water/methanol mixtures confirm that such mixtures can be separated cleanly using this new MOF.

Removing small amounts of water, even though it may not sound so exciting, is one of the thorniest practical problems in many industrial sectors. Separating water/alcohol mixtures is a big challenge in the chemical industry. Such mixtures often form azeotropes, requiring the use of entrainers in extractive distillation processes, and incurring high energy costs. The separation is economically unattractive for removing small amounts of either component, because one must evaporate and condense the entire mixture. Selective adsorption of either water or alcohols using zeolites, activated carbons and polymers offer energy-efficient alternatives, especially for removing trace quantities.[1,2] The performance of any adsorbent is governed by a combination of selectivity and uptake capacity.[3]

Another example where porous materials are used as selective adsorbents is the drying of gases, for example, air drying in medium- and heavy-duty commercial vehicles.[4] The desiccant is usually silica gel or zeolites. The latter are preferred because they are cheaper and regenerable, ensuring drying performance. Their main disadvantage is the high temperature required for regeneration.

Similarly, small amounts of water in diesel cause problems in fuel injection systems. Water leads to corrosion, reduced lubricity and microbe growth. It must be removed before the fuel entering the injection system.[5] The filters in diesel engines achieve 99% separation efficiency.[5] For the final 1%, an additional drying unit is required. Here, again, adsorbents come into play.

Metal–organic frameworks (MOFs)[6–8] are a new class of porous materials whose surface area, pore structure and thermal stability depend strongly on their individual components. This makes them interesting for selective molecular separations. MOFs can separate molecules through either physical sieving or on the basis of chemical affinity and even chemical bonding.[9,10] Some MOFs can separate different molecules by commensurate adsorption,[11] wherein the number of molecules adsorbed per unit cell relates to the symmetry of the framework and its topology.

Several MOFs have been studied for their water up-take properties and some of them show promising water vapour stability.[12–21] Among these, zirconium[20] and pyrazolate[19] MOFs show the highest water stability and capacity. Searching for new water-stable MOFs, we focused on lanthanide-based materials. This is because the large coordination spheres and flexible coordination geometries of lanthanide ions can facilitate structural re-organization without disrupting the overall framework.[22,23] Here, we report the synthesis and characterization of a new lanthanum MOF with a highly hydrophilic framework. This MOF is thermally and chemically stable up to 300 °C. Subsequently, we show that it is highly selective in water adsorption, making it an excellent material for drying air and for water-alcohol separations.

A mixture of $La(NO_3)_3\cdot 6H_2O$ and pyrazine-2,5-dicarboxylic acid (Hpyzdc) reacted in a molar ratio of 1.5:1 in H_2O, forming a crystalline white product at 120 °C. Single-crystal XRD reveal that this compound has the general formula $[La(pyzdc)_{1.5}$-

[a] R. Plessius, R. Kromhout, Dr. A. L. D. Ramos, Dr. M. C. Mittelmeijer-Hazeleger, Prof. R. Krishna, Prof. G. Rothenberg, Dr. S. Tanase
Van 't Hoff Institute for Molecular Sciences, University of Amsterdam, Science Park 904, 1098 XH Amsterdam (The Netherlands)
E-mail: s.grecea@uva.nl

[b] Dr. A. L. D. Ramos
Environmental Engineering Department, Federal University of Sergipe (UFS) (Brazil)

[c] Dr. M. Ferbinteanu
Faculty of Chemistry, Inorganic Chemistry Department, University of Bucharest, Dumbrava Rosie 23, Bucharest 020462 (Romania)

Supporting information for this article is available on the WWW under http://dx.doi.org/10.1002/chem.201403241.

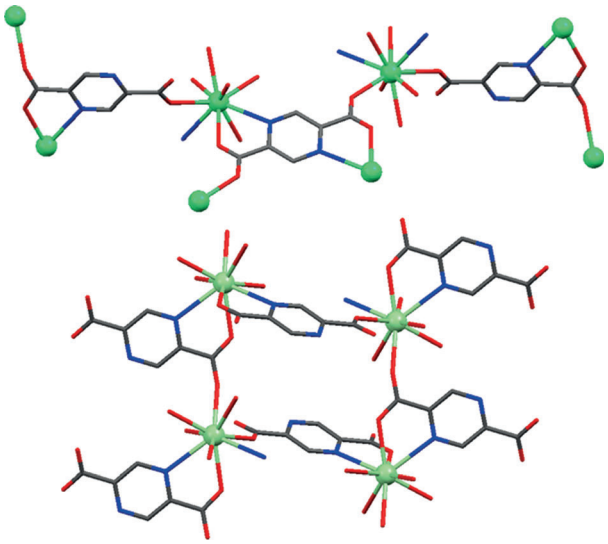

Figure 1. Representation of the coordination modes of the ligand (top) and the tetranuclear SBU (bottom).

$(H_2O)_2]\cdot 2H_2O$ (Table S1 in the Supporting Information). In the asymmetric unit, the La^{III} ion is surrounded by five fully deprotonated pyrazine-2,5-dicarboxylate ($pyzdc^{2-}$) ligands and two water molecules. The $pyzdc^{2-}$ ligand adopts two coordination modes: hexadentate, bridging four La^{III} ions, and tetradentate, linking three La^{III} ions (Figure 1). This hexadentate ligand bridges $[La(pzdc)_{1.5}(H_2O)_2]$ units, creating tetranuclear secondary building-units (SBU). These are linked by the tetradentate ligand, creating a 3D network structure. This is a microporous structure with hydrophilic 1D tetragonal channels that accommodate the water molecules (Figure 2). The window size of the

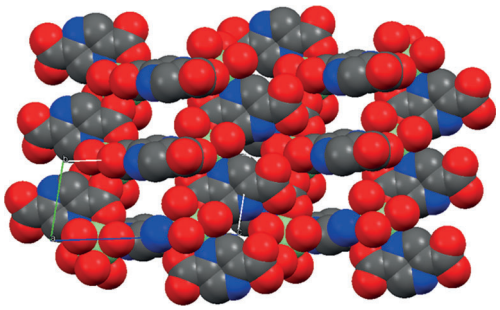

Figure 2. Space-filling representation of the 3D structure of $[La(pyzdc)_{1.5}(H_2O)_2]\cdot 2H_2O$. Non-coordinated water molecules were removed for clarity

framework is 3.8×3.5 Å. The shortest distance between two La^{III} ions is 6.381 Å. For the hexadentate $pyzdc^{2-}$ ligand, the dihedral angle between the pyrazine ring and the carboxylate group is 14.02°. Conversely, the tetradentate ligand has a monodentate carboxylate group which is less planar; the dihedral angle is 27.69°. The average La–O and La–N bond distances are 2.433 and 2.656 Å, respectively, agreeing with earlier reports.[24,25]

A robust metal–organic framework must withstand high temperatures to evacuate solvent molecules from its framework yet still retain its structure. We therefore ran a thermogravimetric analysis (TGA) of the LaMOF between 25–700 °C (Figure 3). We found that this MOF is stable up to 400 °C. The first step in the TGA from 25 °C to 150 °C corresponds to the removal of one lattice water molecule and one coordinated water molecule (weight loss ca. 5.6%, calculated 5.9%). The next step from 150 °C to about 300 °C corresponds to the second coordinated water molecule (weight loss ca. 4.4%, calculated 3.9%). This indicates a general formula $[La(pyzdc)_{1.5}(H_2O)_2]\cdot 0.5H_2O$. Note that 1.5 moles of lattice water molecules are lost by the framework when it is separated from the mother solution. This supports the highly disordered state of the water molecules accommodated in the channels (observed by single-crystal XRD). The PXRD pattern of the bulk material confirms the retention of the framework after the loss of the 1.5 lattice water molecules (Figure S3 in the Supporting Information).

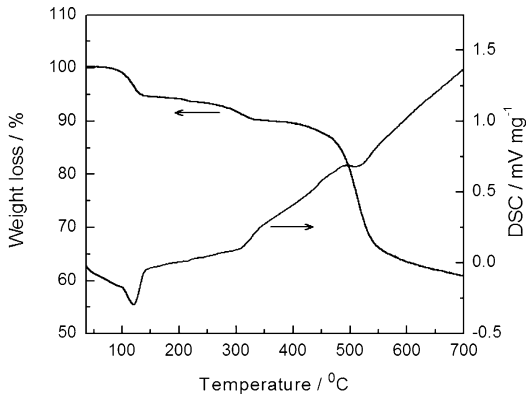

Figure 3. TGA and DSC curves of $[La(pyzdc)_{1.5}(H_2O)_2]\cdot 2H_2O$ measured in oxygen atmosphere and at 3 °C min^{-1}.

The framework starts decomposing at about 400 °C and the organic ligand removal is complete above 600 °C, when the lanthanide oxide is formed. To check the stability of our MOF, we ran XRD measurements after heating the samples at 200 °C for 3 h (Figure S4 in the Supporting Information). The XRD patterns of the original LaMOF and of the evacuated sample are almost identical, although some diffraction peaks are less intense. It suggests that either crystallinity is partially lost or that rearrangements occur upon dehydration. However, the general structural integrity of the LaMOF is unaltered upon water removal (see below). In contrast, the XRD pattern of the activated Pr and Nd MOFs are completely different from the pristine samples (see Supporting Information for details). This indicates that both MOF frameworks undergo significant changes upon dehydration. We can explain these differences by the geometrical configuration of the SBUs (see Supporting Information for details). The presence of a rich hydrogen bonding network (in which the water molecules play a key role) stabilizes the tetragonal channels in LaMOF and the hexagonal channels in Pr and NdMOFs. Accessible voids are created once the water molecules are removed. Thus, the hexagonal channels are more prone to structural rearrangements than the tetragonal ones.

Importantly, our LaMOF shows also an excellent hydrothermal stability. Treating the crystalline compound with boiling

water or toluene for 72 h does not result in loss of crystallinity (Figure S6 in the Supporting Information). This is unusual, as most MOFs are unstable at high humidity. The stability is due to the presence of the highly hydrophilic tetragonal channels with a face-to-face arrangement of the pyzdc ligand within the SBUs. Such structural stability against water is rare in MOFs.[26–30]

Encouraged by the presence of highly disordered water molecules, which leave the 1D tetragonal channels without perturbing the overall 3D structure, we tested the water adsorbent properties of our LaMOF. We first focused on the water adsorption from air. Thus, we activated the LaMOF by heating at 200 °C for 24 h and then exposed the MOF at ambient conditions. The XRD patterns of the samples exposed to air are the same as for the pristine compound (Figure 4), indicating water adsorption from the atmosphere. The TGA shows that one water molecule was retained per unit cell after 72 h exposure (Figure 5). We ascribe this to the highly hydrophilic nature of the LaMOF. The activation and air exposure experiments can be repeated 12 cycles with no change, confirming that LaMOF is robust to dehydration/hydration. This material is a good desiccant for air drying.

We also measured the adsorption isotherms for the fully desolvated samples. The N_2 isotherms at 77 K showed almost no adsorption. But, the N_2 molecules (kinetic diameter 3.64 Å) are too large for the MOF channels. Using CO_2 instead (kinetic diameter 3.30 Å), we saw a small adsorbed amount (ca. 3 cm^3g^{-1}). We then performed vapour-adsorption studies for water and methanol. Water is significantly smaller than nitrogen (its kinetic diameter is only 2.75 Å) and can access the MOF's micropores.

Indeed, our MOF adsorbs water selectively (Figure 6). Water adsorbs gradually in the low pressure range. Its uptake increases as the vapour pressure increases, reaching 1.2 mmol g^{-1} of MOF. The adsorption is faster in the low pressure range because water forms hydrogen bonds to the framework and the rearrangement energy is low.[31] Although the channels are hydrophilic, they are too narrow for molecules other than water. This is confirmed by the methanol adsorption experiments (Figure 6).

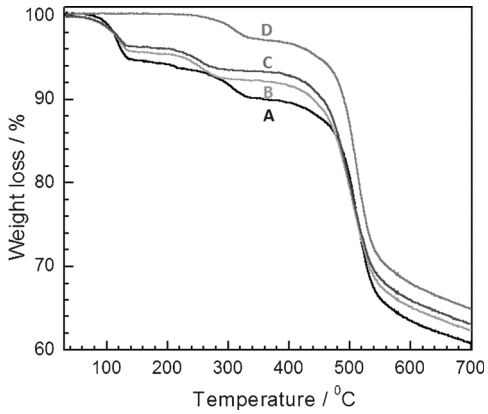

Figure 4. TGA and DSC curves of $[La(pyzdc)_{1.5}(H_2O)_2]\cdot 0.5\,H_2O$ as synthesized (A), activated at 200 °C (D), after 24 h air exposure (C) and after 72 h air exposure (B).

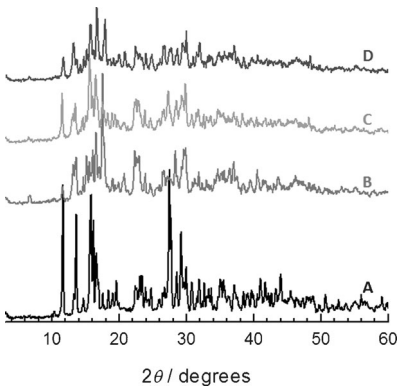

Figure 5. The powder XRD of $[La(pyzdc)_{1.5}(H_2O)_2]\cdot 0.5\,H_2O$ as synthesized (A), activated at 200 °C (B), after 96 h air exposure (C) and after 59 days air exposure (D).

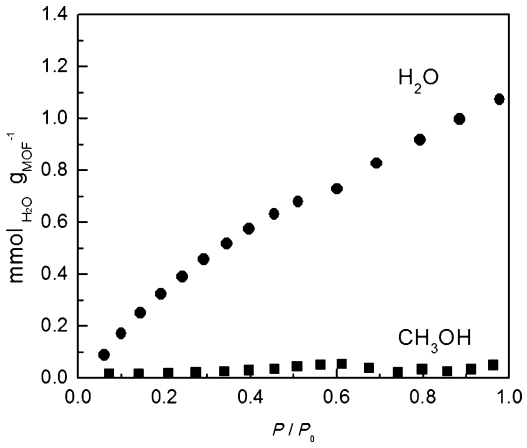

Figure 6. Water (circles) and methanol (squares) adsorption isotherms of $[La(pyzdc)_{1.5}(H_2O)_2]\cdot 0.5\,H_2O$ activated at 200 °C.

The selective water adsorption is consistent with the observed aperture size of 3.8 × 3.5 Å. Such selective adsorption of water over other molecules is reported very rarely in literature.[31–36] To the best of our knowledge, this is the first lanthanide MOF showing highly selective water adsorption. The robustness of the frameworks is also confirmed by the water adsorption. The isotherms are practically identical after three consecutive activation–uptake cycles (Figure S8 in the Supporting Information). Transient uptake measurement experiments (Figure S9 in the Supporting Information) indicate that the intracrystalline diffusivities in LaMOF are of the order of 10^{-14} m^2s^{-1}; this value is lower than that reported for LTA-4A zeolite by an order of magnitude, because of the stronger constraints within the narrow channels. Any adsorbed water is easily removed at 200 °C. Transient breakthrough simulations for water/alcohol mixture confirm that water/alcohol mixtures can be separated cleanly using our lanthanum MOF (see Supporting Information for details).

This new lanthanide MOF, $[La(pyzdc)_{1.5}(H_2O)_2]\cdot 2H_2O$, is a highly unusual material. It has a stable microporous structure with hydrophilic 1D tetragonal channels having a window size appropriate for accommodating water molecules. Unlike most MOFs, it is also hydrothermally stable at high temperatures. As far as we know, this is the first lanthanide MOF showing highly selective water adsorption. It opens exciting opportunities for developing desiccants for removing small amounts of water from water/alcohol mixtures as well as wet gases.

Acknowledgement

A.L.D.R. acknowledges CAPES Foundation for his senior fellowship under the Program "Science without Borders". M.F. acknowledges support from PNII UEFISCDI PCCE 9/2010 research grant.

Keywords: adsorption · desiccant · lanthanides · metal–organic frameworks

[1] A. F. P. Ferreira, M. C. Mittelmeijer-Hazeleger, M. A. Granato, V. F. D. Martins, A. E. Rodrigues, G. Rothenberg, *Phys. Chem. Chem. Phys.* **2013**, *15*, 8795.
[2] E. J. Ras, M. J. Louwerse, M. C. Mittelmeijer-Hazeleger, G. Rothenberg, *Phys. Chem. Chem. Phys.* **2013**, *15*, 4436.
[3] R. Krishna, J. R. Long, *J. Phys. Chem. C* **2011**, *115*, 12941.
[4] W. K. Park, S. D. Mun, H. K. Lee, G. E. Yang, *Int. J. Automot. Technol.* **2011**, *12*, 705.
[5] B. Elvers, *Handbook of fuels*, Wiley-WCH, Weinheim, **2008**.
[6] D. Farrusseng, *Metal–Organic Frameworks*, Wiley-VCH, Weinheim, **2011**.
[7] D. Farrusseng, S. Aguado, C. Pinel, *Angew. Chem.* **2009**, *121*, 7638; *Angew. Chem. Int. Ed.* **2009**, *48*, 7502.
[8] M. Schroder, *Topics Curr. Chem.* **2010**, *293*, 1-295.
[9] J. Z. Gu, W. G. Lu, L. Jiang, H. C. Zhou, T. B. Lu, *Inorg. Chem.* **2007**, *46*, 5835.
[10] M. Shah, M. C. McCarthy, S. Sachdeva, A. K. Lee, H. K. Jeong, *Ind. Eng. Chem. Res.* **2012**, *51*, 2179.
[11] X. Wu, Z. H. Lin, C. He, C. Y. Duan, *New J. Chem.* **2012**, *36*, 161.
[12] J. Ehrenmann, S. K. Henninger, C. Janiak, *Eur. J. Inorg. Chem.* **2011**, 471.
[13] P. Ghosh, K. C. Kim, R. Q. Snurr, *J. Phys. Chem. C* **2014**, *118*, 1102.
[14] S. K. Henninger, H. A. Habib, C. Janiak, *J. Am. Chem. Soc.* **2009**, *131*, 2776.
[15] S. K. Henninger, F. Jeremias, H. Kummer, C. Janiak, *Eur. J. Inorg. Chem.* **2012**, 2625.
[16] F. Jeremias, A. Khutia, S. K. Henninger, C. Janiak, *J. Mater. Chem.* **2012**, *22*, 10148.
[17] S. Paranthaman, F. X. Coudert, A. H. Fuchs, *Phys. Chem. Chem. Phys.* **2010**, *12*, 8123.
[18] A. Rezk, R. Al-Dadah, S. Mahmoud, A. Elsayed, *Int. J. Heat Mass Transfer* **2012**, *55*, 7366.
[19] C. R. Wade, T. Corrales-Sanchez, T. C. Narayan, M. Dinca, *Energy Environ. Sci.* **2013**, *6*, 2172.
[20] H. Furukua, F. Gandara, Y. B. Zhang, J. Jiang, W. L. Queen, R. Hudson, O. M. Yaghi, *J. Am. Chem. Soc.* **2014**, *136*, 4369.
[21] F. Jeremias, D. Frohlich, C. Janiak, S. K. Henninger, *New J. Chem.* **2014**, *38*, 1846.
[22] Y. B. He, R. Krishna, B. L. Chen, *Energy Environ. Sci.* **2012**, *5*, 9107.
[23] S. C. Xiang, Y. B. He, Z. J. Zhang, H. Wu, W. Zhou, R. Krishna, B. L. Chen, *Nat. Commun.* **2012**, *3*, 954.
[24] X. J. Zheng, L. P. Jin, *J. Chem. Crystallogr.* **2005**, *35*, 865.
[25] P. Yang, J. Z. Wu, Y. Yu, *Inorg. Chim. Acta* **2009**, *362*, 1907.
[26] K. A. Cychosz, A. J. Matzger, *Langmuir* **2010**, *26*, 17198.
[27] M. Kandiah, M. H. Nilsen, S. Usseglio, S. Jakobsen, U. Olsbye, M. Tilset, C. Larabi, E. A. Quadrelli, F. Bonino, K. P. Lillerud, *Chem. Mater.* **2010**, *22*, 6632.
[28] S. J. Yang, C. R. Park, *Adv. Mater.* **2012**, *24*, 4010.
[29] J. Duan, M. Higuchi, R. Krishna, T. Kiyonaga, Y. Tsutsumi, Y. Sato, Y. Kubota, M. Takata, S. Kitagawa, *Chem. Sci.* **2014**, *5*, 660.
[30] J. Duan, M. Higuchi, S. Horike, M. L. Foo, K. P. Rao, Y. Inubushi, T. Fukushima, H. Kitagawa, *Adv. Funct. Mater.* **2013**, *23*, 3525.
[31] A. Shigematsu, T. Yamada, H. Kitagawa, *J. Am. Chem. Soc.* **2012**, *134*, 13145.
[32] B. L. Chen, Y. Y. Ji, M. Xue, F. R. Fronczek, E. J. Hurtado, J. U. Mondal, C. D. Liang, S. Dai, *Inorg. Chem.* **2008**, *47*, 5543.
[33] G. F. de Lima, A. Mavrandonakis, H. A. de Abreu, H. A. Duarte, T. Heine, *J. Phys. Chem. C* **2013**, *117*, 4124.
[34] T. K. Maji, K. Uemura, H. C. Chang, R. Matsuda, S. Kitagawa, *Angew. Chem.* **2004**, *116*, 3331; *Angew. Chem. Int. Ed.* **2004**, *43*, 3269.
[35] K. Zhang, R. P. Lively, M. E. Dose, A. J. Brown, C. Zhang, J. Chung, S. Nair, W. J. Koros, R. R. Chance, *Chem. Commun.* **2013**, *49*, 3245.
[36] K. Zhang, R. P. Lively, C. Zhang, W. J. Koros, R. R. Chance, *J. Phys. Chem. C* **2013**, *117*, 7214.

Received: April 25, 2014
Published online on May 27, 2014

CHEMISTRY
A European Journal

Supporting Information

Highly Selective Water Adsorption in a Lanthanum Metal–Organic Framework

Raoul Plessius,[a] Rosa Kromhout,[a] André Luis Dantas Ramos,[a, b] Marilena Ferbinteanu,[c] Marjo C. Mittelmeijer-Hazeleger,[a] Rajamani Krishna,[a] Gadi Rothenberg,[a] and Stefania Tanase*[a]

chem_201403241_sm_miscellaneous_information.pdf

Experimental Section

In a typical reaction, 0.6 mmol of $La(NO_3)_3 \cdot 6H_2O$, 0.9 mmol of pyrazine-2,5-dicarboxylic acid (pyzdc) and 15 ml water were heated at 120 ^oC for 48 h. A white highly crystalline insoluble material is formed. This is separated by filtration, washed with water and ethanol and dried in air. The purity of the compound was also confirmed by the comparison of the experimental powder X-ray diffraction patterns to those calculated from the single X-ray data.
$[La(pyzdc)_{1.5}(H_2O)_2] \cdot 0.5H_2O$: yield 220 mg (79 %). Analysis calculated: C 24.65, H 1.84, N 9.58; found: C 24.95, H 2.01, N 9.65. IR (cm^{-1}): 3213 br, 3136 w, 1591 s, 1555 s, 1473 m, 1386 s, 1314 s, 1181 s, 1037 s, 934 m, 827 s, 765 s, 514 s, 477 m, 456 m.

Chemicals were purchased from Aldrich and were used without further purification. IR spectra (4000-400 cm^{-1}, resolution 0.5 cm^{-1}) were recorded on a Varian 660 FTIR spectrometer equipped with a Gladi ATRTR device, using the reflectance technique. TGA measurements were performed using a STA 449 F3 Jupiter® (NETZSCH Instrument) unit. The measurements were done in an oxygen atmosphere with a flow of 40ml/min. PXRD measurements were carried out on a Rigaku Miniflex X-ray Diffractometer. Measurements were done from 3^o to 90^o with a turning speed of 5^o/min. The particle size analysis was performed with PDXL2 Rigaku data analysis software and it indicates existence of crystallites of 15–20 μm. Nitrogen adsorption experiments at 77 K were performed on a Thermo Scientific Surfer instrument. Water and methanol sorption experiments as well as kinetic uptake measurements were performed in a micro-calorimeter (Calvet C80, Setaram) which can operates isothermally and is connected to a home built manometric apparatus (Figure S1). Blank experiments were carried out at 293 K by introducing a known amount of gas into the empty sample holder and measure the final pressure. To calculate the amount adsorbed, the blank curves are used with a correction for the volume occupied by the MOF sample itself. The sample is outgassed at 473 K for 6 hours before any adsorption measurements. The holder containing the adsorptive was placed in a thermostatic bath; its temperature was set to 273 K and the desired pressure was obtained. At t = 0 the valves of the introduction system were opened and the change in weight was followed by a Rubotherm balance. For a crystal of radius r_c, the expression for fractional approach to equilibrium is:

$$\frac{\bar{q}_i(t)}{q_i(r_c, t=\infty)} = 1 - \frac{6}{\pi^2}\sum_{m=1}^{\infty}\frac{\exp(-m^2\pi^2\frac{D_i}{r_c^2}t)}{m^2}$$

This equation allows data on transient uptake to be fitted to obtain an average value of the Fick diffusivity D_i. The experimentally measured transient uptake of water could be fitted reasonably accurately taking $\frac{D_i}{r_c^2}$ = 3.5×10^{-4} s^{-1}. The size range of crystals used in these experiments was 15 – 25 μm. This results in values of intra-crystalline diffusivities in the range 2×10^{-14} m^2 s^{-1} – 3.5×10^{-14} m^2 s^{-1}. These water diffusivity values are about one order of magnitude lower than reported in the literature for LTA-4A zeolite.[1] The lower diffusivity value is to be expected because of the narrow channels of LaMOF.

A colourless prism crystal of $C_9H_7LaN_3O_{10}$ having approximate dimensions of 0.300×0.100×0.100 mm was mounted on a glass fibre. All measurements were made on a Rigaku CCD diffractometer using graphite monochromated Mo-Kα radiation. The data were collected at a temperature of 20±1 °C using the ϖ scan technique to a maximum 2θ value of 54.9°. Omega scans of several intense reflections, made prior to data collection, had an average width at half-height of 0.00° with a take-off angle of 6.0°. Scans of (0.00 + 0.00 tan θ)° were made at a speed of 0.0°/min (in ϖ). The weak reflections (I < 0.0s(I)) were rescanned (maximum of 72 scans) and the counts were accumulated to ensure good counting statistics. Of the 8647 reflections that were collected, 2939 were unique (R_{int} = 0.0264). No decay correction was applied. The linear absorption coefficient, μ, for Mo-K_α radiation is 33.704 cm^{-1}. An empirical absorption correction was applied which resulted in transmission factors ranging from 0.494 to 0.714. The data were corrected for Lorentz and polarization effects. The structure was solved by direct methods[2] and expanded using Fourier techniques. The non-hydrogen atoms were refined anisotropically. Some hydrogen atoms were refined isotropically and the rest were refined using the riding model. All calculations were performed using the CrystalStructure[3] crystallographic software package except for refinement, which was performed using SHELXL-97.[2] Crystallographic data have been submitted to Cambridge Structural Data Base and registered as CCDC 973063.

Synthesis of the Ln-MOFs (Ln = La, Pr, Nd)

We found that the reaction temperature and the lanthanum source are crucial. An earlier reported compound, $[La(pyzdc)_{1.5}(H_2O)]$, was obtained by reacting $LaCl_3{\cdot}7H_2O$ and H_2pzdc at 160 °C for 72 h. This gives a different structure, a non-porous material in which each La(III) ion is surrounded by six $pzdc^{2-}$ ligands and one water molecule.[4]

Moreover, we performed the hydrothermal reaction between $Ln(NO_3)_3{\cdot}6H_2O$ (Ln = Pr, Nd) and 2,5-pyrazinedicarboxylic using similar conditions as for the lanthanum analogue. The products are $[Ln(pyzdc)_{1.5}(H_2O)_3]{\cdot}H_2O$ (Ln = Pr, Nd) and our XRD analysis shows that they are identical to those obtained earlier by performing a similar reaction at 160 °C.[5] However, the number of lattice water molecules is different. These compounds also have a 3D structure with one-dimensional channels which accommodate water molecules. But here, the lanthanide ion is surrounded by three water molecules and four pzdc linkers.[5] The structure is built from hexanuclear SBU which adopt a chair configuration (see Figure S2). These SBUs are linked by a hexadentate pzdc ligand to create a three-dimensional framework with open channels.[5] The smaller ionic radii of Pr(III) and Nd(III) compared with La(III) are the reason that the first two form hexanuclear SBUs, while La forms tetranuclear ones. Indeed, the Pr and Nd MOFs have only one lattice water molecule per unit cell, whilst the La MOF has two.

The TGAs of the Pr and Nd MOFs showed that the lattice water molecule is removed (*ca.* 3.8 %) up to 150 °C (see Figure S4). The three coordinated water molecules are removed in the 150–300 °C range. Just like the LaMOF, the framework decomposition starts at *ca.* 400 °C.

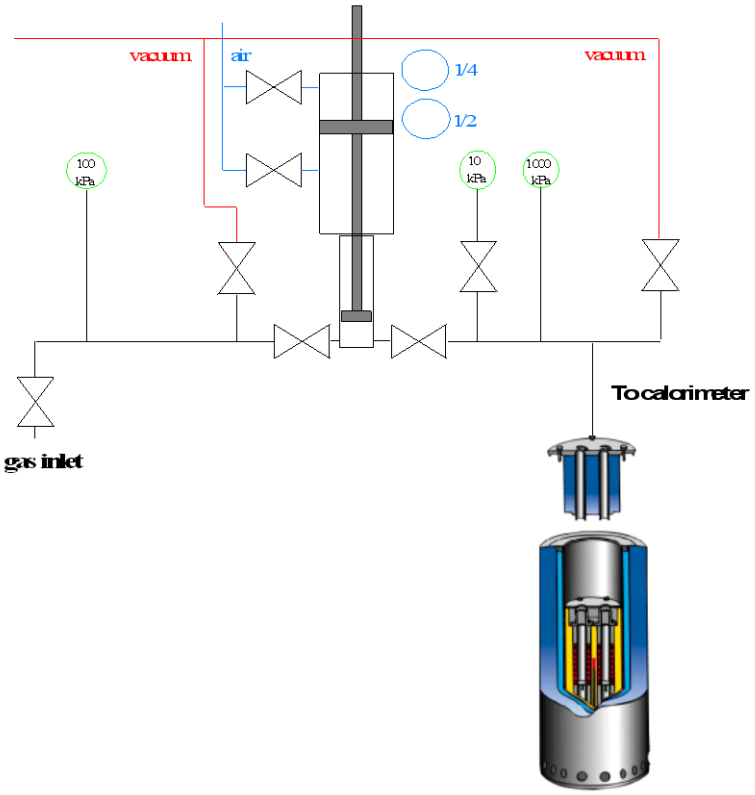

Figure S1. The home-made Setaram Calvet C80 calorimeter.

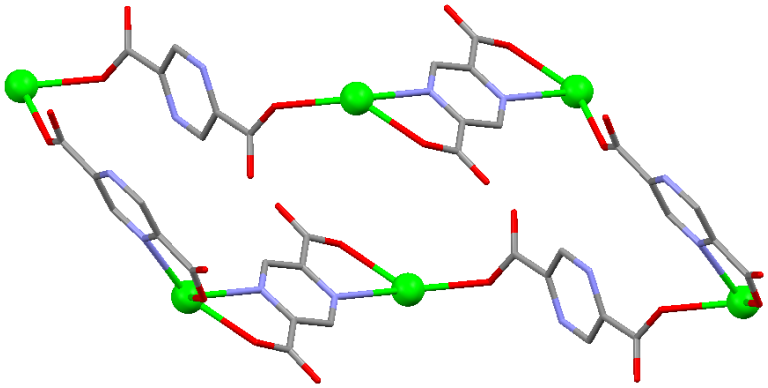

Figure S2. The chair conformation of the hexanuclear SBU of $[Pr(pyzdc)_{1.5}(H_2O)_3]\cdot H_2O$

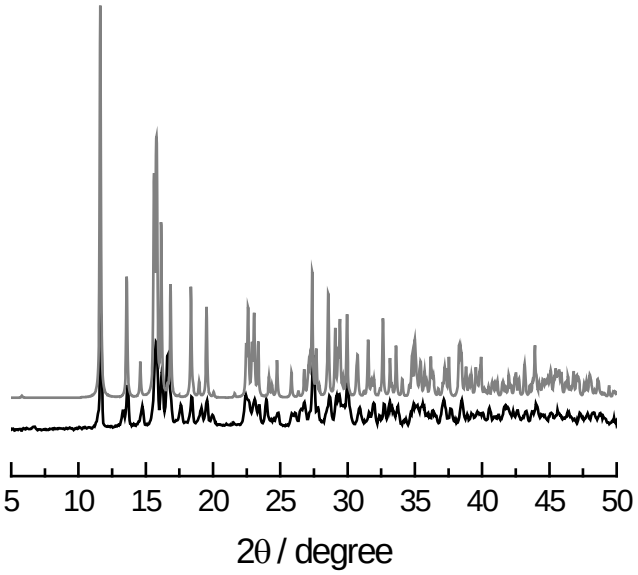

Figure S3. The experimental (black) and simulated (grey) powder XRD pattern of $[La(pyzdc)_{1.5}(H_2O)_2]\cdot xH_2O$

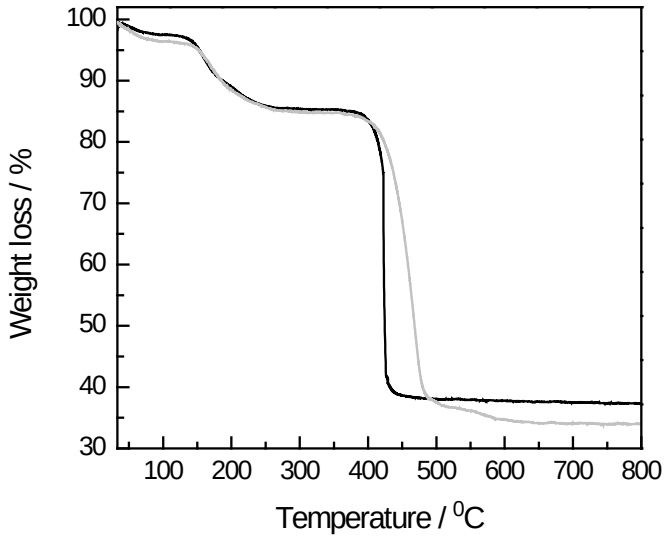

Figure S4. TGA curves of PrMOF (black) and NdMOF (gray) measured in oxygen atmosphere and at 5 ^{o}C/min.

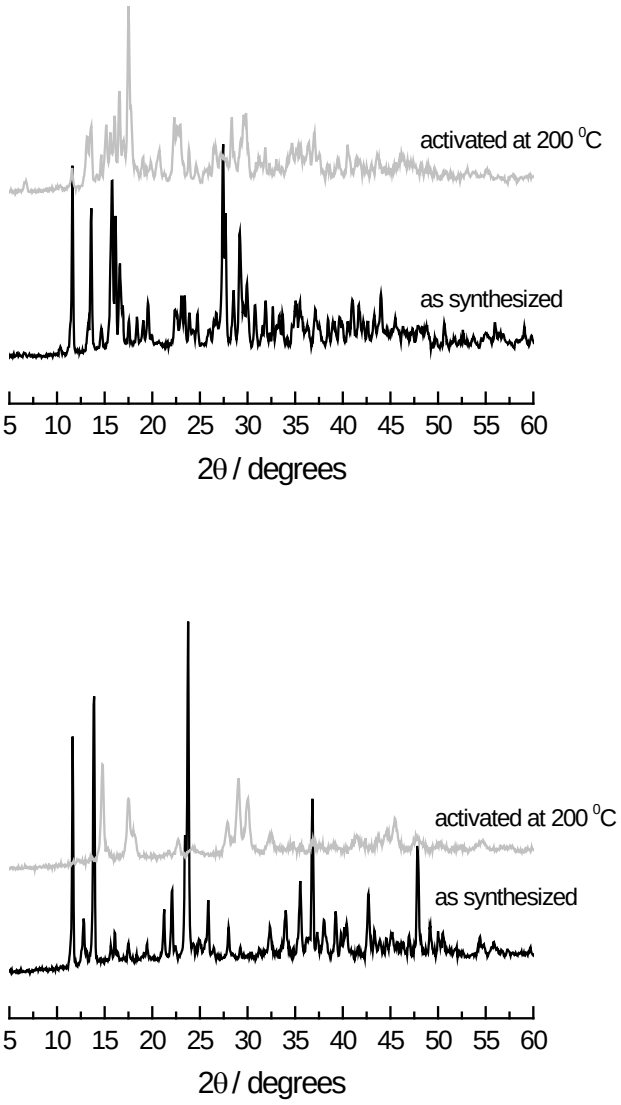

Figure S5. The powder XRD patterns of $[La(pyzdc)_{1.5}(H_2O)_2]\cdot 0.5H_2O$ (top) and $[Pr(pyzdc)_{1.5}(H_2O)_3]\cdot H_2O$ (bottom).

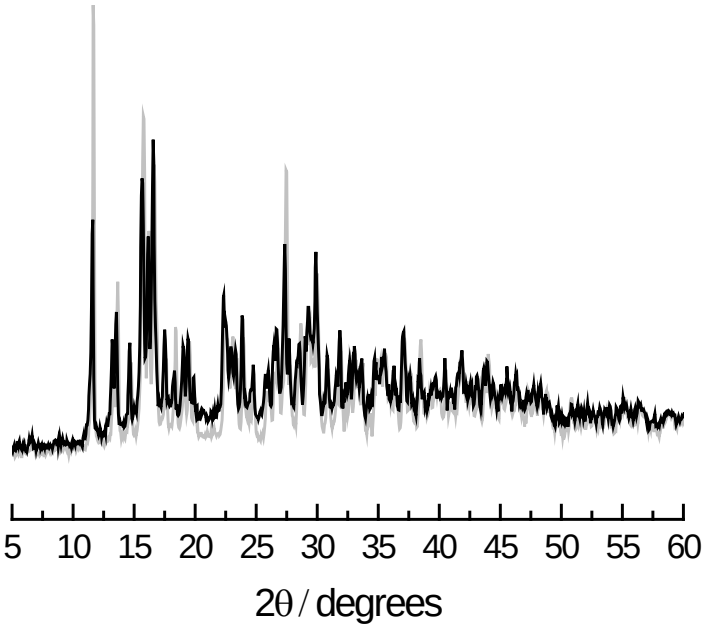

Figure S6. The powder XRD patterns of $[La(pyzdc)_{1.5}(H_2O)_2]\cdot 0.5H_2O$ as synthesized (grey) and after boiling in water for 72 h (black).

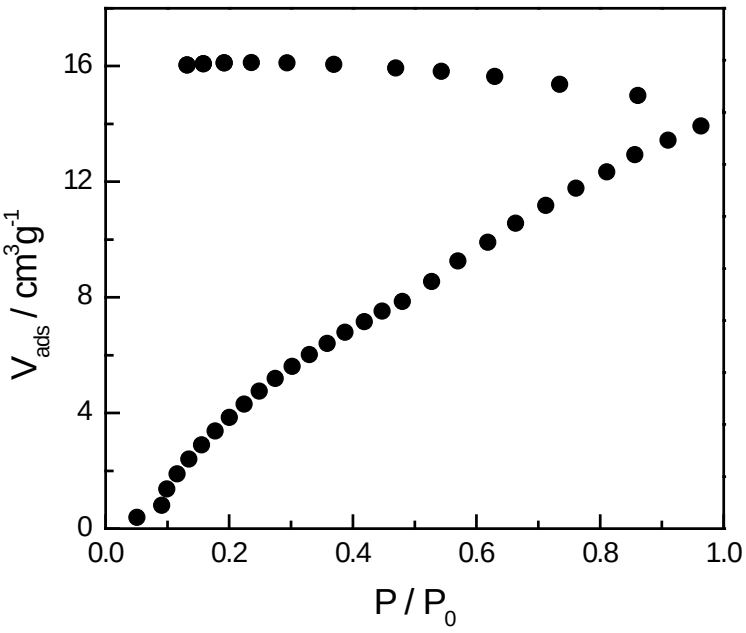

Figure S7. Water adsorption/desorption isotherms of $[La(pyzdc)_{1.5}(H_2O)_2]\cdot 2H_2O$ measured at 25 °C.

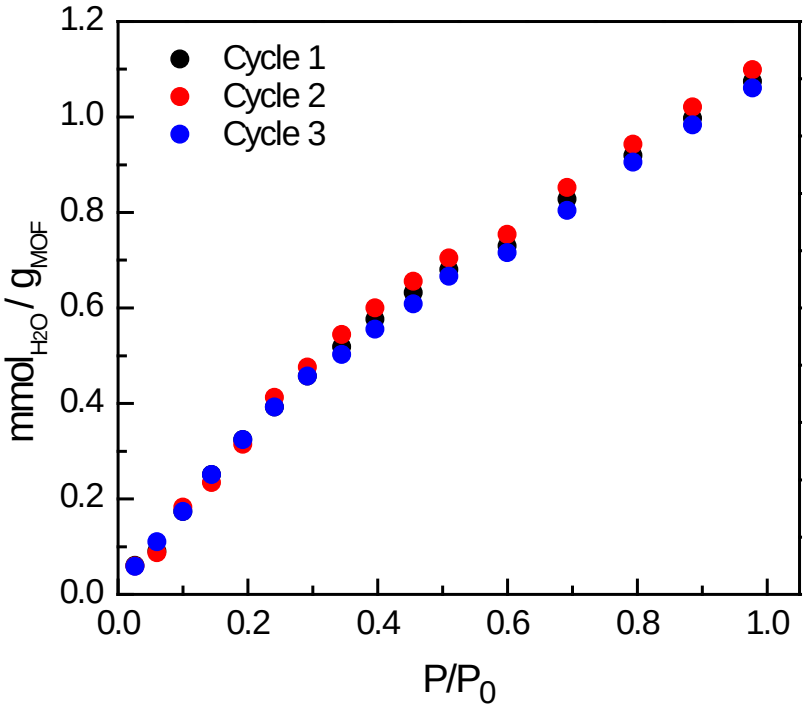

Figure S8. Water adsorption isotherms of $[La(pyzdc)_{1.5}(H_2O)_2]\cdot 2H_2O$ measured for three consecutive activation-uptake cycles.

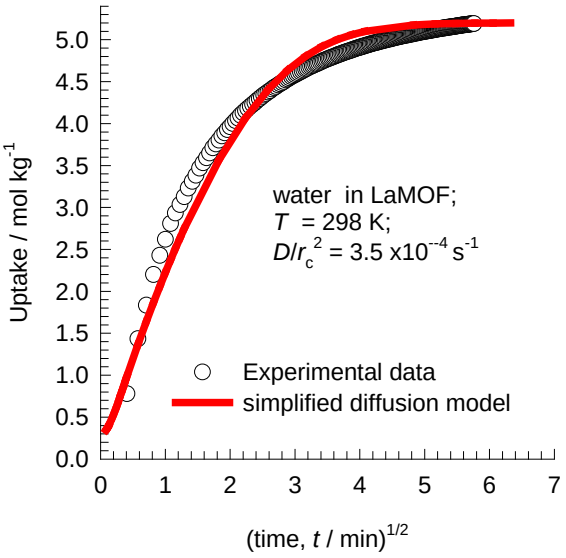

Figure S9. Kinetic water adsorption of $[La(pyzdc)_{1.5}(H_2O)_2]\cdot 2H_2O$ measured at 25 °C. The continuous red line represents the model fit of the experimental data for transient uptake.

Table S1. XRD summary data for $[La(pyzdc)_{1.5}(H_2O)_2]\cdot 2H_2O$

Empirical formula	$C_9H_{11}LaN_3O_{10}$
Formula weight ($gmol^{-1}$)	460.07
Crystal color, Habit	colorless, prism
Crystal dimensions (mm)	0.300×0.100×0.100
Crystal system	triclinic
Lattice type	Primitive
No. of reflections used for unit	8368
Cell determination (2θ range, °)	6.2−55.0
Lattice parameters	a = 6.3773(3) Å b = 6.9719(2) Å c = 15.512(1) Å α = 78.963(6)° β = 87.657(6)° γ = 71.990(5)° V = 643.64(6) $Å^3$
Space group	P_{-1} (#2)
Z value	2
D_{calc} (gcm^{-3})	2.353
F_{000}	438.00
μ(MoKα), cm^{-1}	33.704
Temperature, °C	20.0
R1 (I>2.00σ(I))	0.0225
wR2 (All reflections)	0.0569
Goodness of Fit Indicator	1.118

References

[1] M. Pera-Titus, C. Fité, V. Sebastián, E. Lorente, J. Llorens, F. Cunill, *Ind. Eng. Chem. Res.* **2008**, *47*, 3213.

[2] G. M. Sheldrick, *Acta Cryst.* **2008**, *A64*, 112.

[3] CrystalStructure 4.0: Crystal Structure Analysis Package, Rigaku Corporation (2000-2010). Tokyo 196-8666, Japan.

[4] X. J. Zheng, L. P. Jin, *J. Chem. Cryst.* **2005**, *35*, 865.

[5] P. Yang, J. Z. Wu, Y. Yu, *Inorg. Chem. Acta* **2009**, *362*, 1907.

Pulse chromatographic simulations

In order to demonstrate the efficacy of LaMOF for separation of water/alcohol mixtures we conducted transient breakthrough simulations. The methodology used for these simulations are the same as described in earlier work by Krishna.[1] Experimental validation of the simulation methodology is available in the published literature.[1-6]

Figure S10 shows a schematic of a fixed bed adsorber packed with LaMOF. Assuming plug flow of an water/methanol vapor mixture through a fixed bed maintained under isothermal conditions, the partial pressures in the vapor phase at any position and instant of time are obtained by solving the following set of partial differential equations for each of the species *i* in the gas mixture.

$$\frac{1}{RT}\frac{\partial p_i(t,z)}{\partial t} = -\frac{1}{RT}\frac{\partial\left(v(t,z)\,p_i(t,z)\right)}{\partial z} - \frac{(1-\varepsilon)}{\varepsilon}\rho\frac{\partial \bar{q}_i(t,z)}{\partial t}; \quad i = 1,2 \tag{1}$$

In equation (1), t is the time, z is the distance along the adsorber, ρ is the framework density, ε is the bed voidage, v is the interstitial gas velocity, and $\bar{q}_i(t,z)$ is the *spatially averaged* molar loading within the crystallites of radius r_c, monitored at position z, and at time t.

The *interstitial* gas velocity is related to the *superficial* gas velocity by

$$v = \frac{u}{\varepsilon} \tag{2}$$

For the purpose of these simulations we neglect intra-crystalline diffusional influences and assume the entire crystallite particle can be considered to be in thermodynamic equilibrium with the surrounding bulk gas phase at that time t, and position z of the adsorber

$$\bar{q}_i(t,z) = q_i(t,z) \tag{3}$$

The component loadings $q_i(t,z)$ at the *outer surface* of the crystallites, i.e. at $r = r_c$, are calculated on the basis of adsorption equilibrium with the bulk gas phase partial pressures p_i at that position z and time t. The adsorption equilibrium is calculated on the basis of the IAST, using Langmuir-Freundlich fits of the pure component isotherms. The fit parameters are specified in Table S2.

The following parameter values were used in the simulations: length of packed bed, L = 0.1 m; fractional voidage of packed bed, ε = 0.4; superficial gas velocity at inlet of adsorber, u = 0.04 m/s, framework density of LaMOF, ρ = 1995 kg/m^3.

For a step input of a vapor mixture containing 5% water and 95% methanol, the transient concentrations at the outlet of the fixed bed are shown in Figure S11. The x-axis in Figure S11 is the dimensionless time, $\tau = \frac{tu}{L\varepsilon}$, obtained by dividing the actual time, t, by the characteristic time, $\frac{L\varepsilon}{u}$.

The poorly adsorbed methanol breaks through almost immediately after feed injection, signifying the fact that very little is adsorbed. The breakthrough of water occurs at a significantly later time step.

A video animation of the traverse of the gas phase concentrations of methanol and water along the fixed bed, have been uploaded as ESI. These give a good indication of the capability of LaMOF to separate water/alcohol mixtures.

Notation

b	Langmuir constant, $\mathrm{Pa}^{-\nu}$
c_i	molar concentrations of species *i* in gas mixture, mol m^{-3}
c_{i0}	molar concentrations of species *i* in gas mixture at inlet to adsorber, mol m^{-3}
L	length of packed bed adsorber, m
p_i	partial pressure of species *i* in mixture, Pa
p_t	total system pressure, Pa
q_i	component molar loading of species *i*, mol kg^{-1}
q_{sat}	saturation loading, mol kg^{-1}
t	time, s
T	absolute temperature, K
u	superficial gas velocity in packed bed, m s^{-1}
z	distance along the adsorber, m

Greek letters

ε	voidage of packed bed, dimensionless
ρ	framework density, kg m^{-3}
τ	time, dimensionless

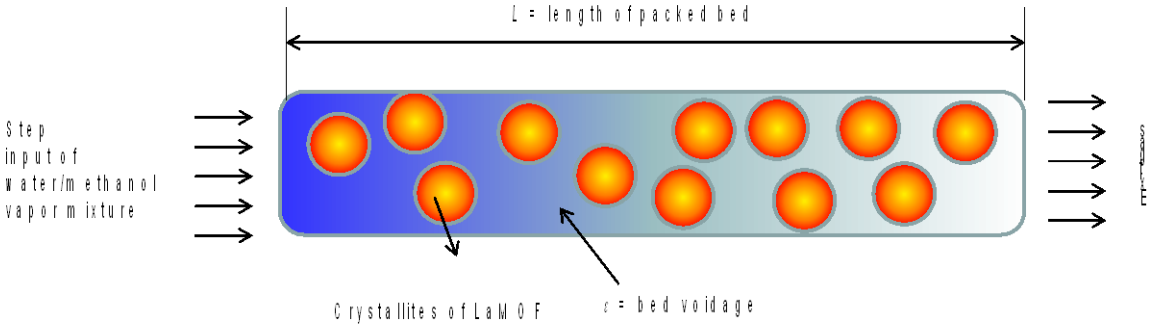

Figure S10. Schematic of a packed bed adsorber packed with LaMOF.

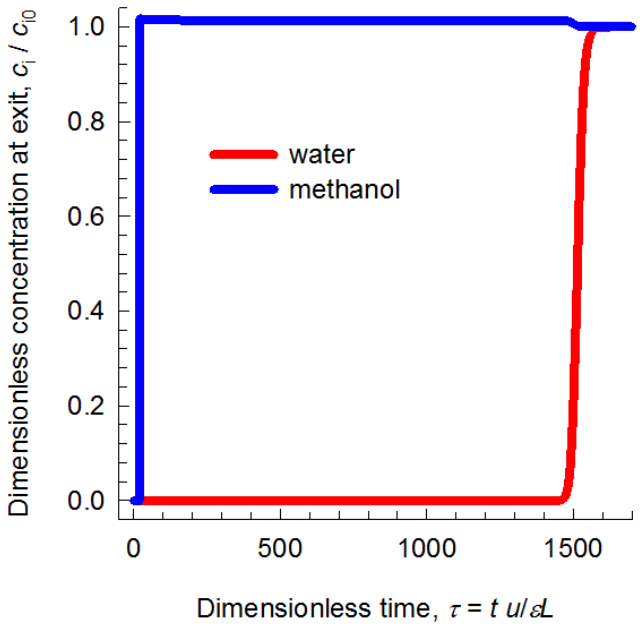

Figure S11. Transient breakthrough simulation results for a feed vapor mixture containing 5% water and 95% methanol. The total pressure is 100 kPa.

Table S2. Langmuir-Freundlich fit parameters for water and methanol in LaMOF at 298 K.

$$q = q_{sat} \frac{bp^{\nu}}{1 + bp^{\nu}}$$

		q_{sat} mol kg^{-1}	b $\mathrm{Pa}^{-\nu}$	ν dimensionless
LaMOF	water	7.9	4.77×10^{-4}	0.73
	methanol	0.56	9.81×10^{-6}	1

References

(1) Krishna, R. The Maxwell-Stefan Description of Mixture Diffusion in Nanoporous Crystalline Materials, *Microporous Mesoporous Mater.* **2014**, *185*, 30-50.

(2) Bloch, E. D.; Queen, W. L.; Krishna, R.; Zadrozny, J. M.; Brown, C. M.; Long, J. R. Hydrocarbon Separations in a Metal-Organic Framework with Open Iron(II) Coordination Sites, *Science* **2012**, *335*, 1606-1610.

(3) Wu, H.; Yao, K.; Zhu, Y.; Li, B.; Shi, Z.; Krishna, R.; Li, J. Cu-TDPAT, an *rht*-type Dual-Functional Metal–Organic Framework Offering Significant Potential for Use in H_2 and Natural Gas Purification Processes Operating at High Pressures, *J. Phys. Chem. C* **2012**, *116*, 16609-16618.

(4) He, Y.; Krishna, R.; Chen, B. Metal-Organic Frameworks with Potential for Energy-Efficient Adsorptive Separation of Light Hydrocarbons, *Energy Environ. Sci.* **2012**, *5*, 9107-9120.

(5) Herm, Z. R.; Wiers, B. M.; Van Baten, J. M.; Hudson, M. R.; Zajdel, P.; Brown, C. M.; Maschiocchi, N.; Krishna, R.; Long, J. R. Separation of Hexane Isomers in a Metal-Organic Framework with Triangular Channels *Science* **2013**, *340*, 960-964.

(6) Yang, J.; Krishna, R.; Li, J.; Li, J. Experiments and Simulations on Separating a CO_2/CH_4 Mixture using K-KFI at Low and High Pressures, *Microporous Mesoporous Mater.* **2014**, *184*, 21-27.